Auto-Ionizing States in the Alkali Atoms with Microsecond Lifetimes*

P. FELDMAN† AND R. NOVICK‡
Columbia Radiation Laboratory, Columbia University, New York, New York

(Received 6 February 1967)

Discrete atomic energy levels lying between the first and second ionization potentials which are metastable against both auto-ionization and radiative decay have been observed in the alkali elements. These levels arise from the excitation of an electron from the outermost closed shell of the atom and have characteristic lifetimes in the microsecond region. A beam of metastable alkali atoms is produced by electron bombardment of neutral ground-state atoms and is detected by collecting the charged products of the decay. Stern-Gerlach magnetic-deflection experiments have been performed to show unambiguously that the signals arise from paramagnetic atoms and not from possible stray-photon effects in the apparatus. The excitation energies, electron-bombardment production cross sections, natural lifetimes, and the tentative spectroscopic assignments of these atoms are listed below:

Element	Energy above ground state (eV)	Tentative assignment	Lifetime (μsec)	Electron-bombardment production cross section (cm^2)
Li	57.3±0.3	$(1s2s2p)^4P$	5.1±1.0	$10^{-(19\pm0.5)}$
Na	31.8±0.3	$(2p^53s3p)^4D$	...	...
K	19.9±0.3	$(3p^54s3d)^4F$	90±20	$10^{-(18\pm0.5)}$
Rb	15.8±0.3	$(4p^55s4d)^4F$	75±20	$10^{-(18\pm0.5)}$
Cs	12.6±0.3	$(5p^56s7s)^4P$ $(5p^56s5d)^4F$ $(5p^56s4f)^4G$	40±15	

The energy and lifetime of the metastable lithium atom are in good agreement with the available theoretical estimates. The metastable states in the heavier alkali atoms are classified in relation to the known I^b spectral terms. Magnetic and electric fields have been found to be effective in reducing the lifetime of the metastable atoms. The Zeeman quenching is discussed in a separate paper. The Stark quenching *rate* has been found to be proportional to the square of the electric field and to increase rapidly with atomic number Z. It is suggested that the Stark quenching results from a second-order interaction which involves the product of the electric field and the spin-orbit or other magnetic operators.

I. INTRODUCTION

IN this paper we report on an experimental study of the properties of the metastable autoionizing states in the alkali atoms.[1] These states have energies appreciably greater than the first ionization energy of the atom; yet they are metastable against both radiative decay and auto-ionization and have lifetimes of the order of 10^{-5} sec. These states are to be contrasted with the short-lived (10^{-15}–10^{-13} sec) auto-ionizing states of the rare-gas atoms and negative ions which have been the subject of recent study in several laboratories.[2,3]

The earliest concern with atomic states metastable against auto-ionization was in connection with attempts to understand the existence of the negative helium ion.[4] The possibility of this ion existing in the lithium-like $(1s^22s)^2S_{1/2}$ ground-state configuration was rejected because variational calculations[5] showed that this state in He^- had a negative binding energy.[6] Ta-You Wu[7] suggested that the $(1s2s2p)^4P_{5/2}$ state of He^- in which two of the electrons are excited could be bound. On the basis of the selection rules,[8] this state was expected to be metastable against radiation and auto-ionization via the Coulomb interaction, and hence could account for the experimental observations. The states which we have investigated are the analogous

* This work was supported in part by the National Aeronautics and Space Administration under Grant No. NsG-360 and in part by the Joint Services Electronics Program (U.S. Army, U.S. Navy, and U.S. Air Force) under Contract No. DA-28-043 AMC-00099(E).

† Present address: E. O. Hulburt Center for Space Research, U.S. Naval Research Laboratory, Washington, D.C. 20390.

‡ Alfred P. Sloan Research Fellow.

[1] P. Feldman and R. Novick, Phys. Rev. Letters **11**, 278 (1963); P. Feldman and R. Novick, in *Atomic Collision Processes*, edited by M. R. C. McDowell (North-Holland Publishing Company, Amsterdam, 1964), pp. 201–210.

[2] C. E. Kuyatt, J. Arol Simpson, and S. R. Mielczarek, Phys. Rev. **138**, A385 (1965). Further references are given in this paper.

[3] U. Fano and J. W. Cooper, Phys. Rev. **138**, A400 (1965).

[4] J. W. Hiby, Ann. Physik **34**, 473 (1939).

[5] Ta-You Wu, Phil. Mag. **22**, 837 (1936).

[6] G. J. Schulz has recently reported the observation of a resonance in the elastic scattering of electrons on helium at 0.45 eV above the He ground state which he attributes to the formation of a compound negative ion state with the configuration $(1s^22s)^2S_{1/2}$. See G. J. Schulz in *Proceedings of the Fourth International Conference on the Physics of Electronic and Atomic Collisions, Quebec, 1965*, edited by L. Kerwin and W. Fite (Science Bookcrafters, Inc., Hastings-on-Hudson, New York, 1965), p. 117.

[7] Ta-You Wu, Phys. Rev. **58**, 1114 (1940).

[8] E. U. Condon and G. H. Shortley, *The Theory of Atomic Spectra* (Cambridge University Press, Cambridge, 1959), p. 371.

$(1s2s2p)^4P_{5/2}$ state in lithium and similar metastable autoionizing states in the other alkali atoms. Dmitriev and co-workers have recently reported evidence for the production of the $(1s2s2p)^4P_{5/2}$ state in N^{+4} and O^{+5}.[9]

We report here on electron-bombardment excitation studies of metastable auto-ionizing states in all of the alkali atoms. These studies include the determination of threshold energies, order-of-magnitude estimates of the absolute production cross sections and time-of-flight determination of the lifetimes of the states. In two cases we have performed an atomic-beam deflection experiment to show unambiguously that the signals are indeed due to atoms and not to photons. We have studied the effect of external fields on these atoms and shown that they can be quenched with both electric and magnetic fields. The magnetic quenching results will be presented in a subsequent paper.[10]

In Sec. II, we consider the selection rules for auto-ionization and deduce the series of spectral terms in the alkalis which are expected to be metastable against autoionization. A survey of available calculations and an examination of related effects is also included. Sections III and IV deal with the apparatus and the procedure employed in our experiments. The results and their interpretation are presented in Sec. V.

II. THEORETICAL CONSIDERATIONS

In this section we consider the interactions which are responsible for auto-ionization transitions, that is, spontaneous transitions from a discrete quantum state to a continuum state of the same energy. From the selection rules and the relative decay rates obtained, the spectral series of states in the alkali atoms which are metastable against auto-ionization and radiation are deduced. We summarize the various calculations to date of energy and lifetime for metastable states in the simplest case, that of the three-electron system. Finally, we consider the problem of excitation to these metastable states and the effects of the breakdown of L–S coupling and external fields on these states.

A. Selection Rules, Energy Levels, and Decay Rates

A discrete atomic state whose energy is greater than the first atomic ionization potential may make a radiationless transition to a continuum state of the same energy. The final continuum state consists of a free electron and an atomic ion in either the ground state or an excited level. In the case of the metastable alkali atoms, the initial discrete state may be formed by the excitation of a *single* electron from the outermost filled shell.

It is convenient to discuss these states in terms of a fictitious rigorously bound stable discrete state ψ_d which is formed by neglecting those terms in the Hamiltonian which couple the state to the continuum. According to time-independent perturbation theory, the first-order rate for a transition from this discrete state with energy E_d to a continuum state ψ_c of energy E_c is given by

$$P^{(1)}=(2\pi/\hbar)|\langle\psi_c\,|\,\mathcal{H}'\,|\,\psi_d\rangle|^2\delta(E_d-E_c), \qquad (1)$$

where $\mathcal{H}'$ is the perturbation coupling the discrete and continuum states and may be either the electrostatic or magnetic interaction between the atomic electrons. In cases where the first-order matrix element vanishes, the second-order transition rate is given by

$$P^{(2)}=\frac{2\pi}{\hbar}\left|\sum_i\frac{\langle\psi_c\,|\,\mathcal{H}'\,|\,\psi_i\rangle\langle\psi_i\,|\,\mathcal{H}'\,|\,\psi_d\rangle}{E_i-E_d}\right|^2\delta(E_d-E_c), \qquad (2)$$

where the summation is over all intermediate states ψ_i.

In general, auto-ionization, as commonly referred to in the literature, is the result of the electrostatic interaction between electrons. The problem of properly evaluating the transition rates for such allowed auto-ionization transitions has been treated by several authors from different points of view.[11] Typical auto-ionization rates via the Coulomb interaction range from 10^{13}–10^{15} sec^{-1}.

If the matrix element of the Coulomb operator connecting a given discrete state to the continuum vanishes, then that state is "metastable" against decay by auto-ionization. The metastable state may decay either by a radiative transition to a lower-lying atomic state or by auto-ionization via one of the weaker magnetic interactions. Second-order processes are also possible when the magnetic interactions couple the metastable state to a short-lived auto-ionizing state.

It is convenient to tabulate the selection rules for nonradiative transitions via the various magnetic interactions along with their relative transition rates. If the spin-orbit terms are negligible compared with the electrostatic repulsion, then Russell-Saunders coupling may be used. It should be noted that in the case of states which are stable against both Coulomb auto-ionization and radiation, it is possible to obtain Hartree–Fock and variational wave functions to use in calculating the matrix elements for the magnetic interactions as well as the energy of the state.

The continuum state is described in the same manner as the discrete state by specifying the spin and angular-momentum quantum numbers for the state of the resulting ion and free electron. The free electron, although moving in an open orbit, has a definite angular momentum with respect to the center of mass of the system, which when added to the angular momentum of the ion, gives the total angular momentum of the

[9] I. S. Dmitriev, D. I. Vinogradova, V. S. Nikolaev, and B. M. Popov, JETP Pis'ma v Radaktslyu **3**, 35 (1966) [English transl.: JEPT Letters **3**, 20 (1966)]. Manson has recently shown that the lifetimes observed by these workers are consistent with the theoretically predicted values for lithium-like metastable auto-ionizing atomic states. See S. T. Manson, Phys. Letters **23**, 315 (1966).

[10] P. Feldman, M.Levitt, R. Novick, and G. Sprott (to be published).

[11] E. Holøien, Phys. Norvegica **1**, 53 (1961); P. G. Burke and H. M. Schey, Phys. Rev. **126**, 147 (1962).

TABLE I. Selection rules for auto-ionization.

Interaction	ΔL	ΔS	ΔJ	Parity change	Relative transition rate[a]
Coulomb	0	0	0	No	1
Spin-orbit Spin–other-orbit	$0, \pm 1$	$0, \pm 1$	0	No	α^4
Spin-spin	$0, \pm 1, \pm 2$	$0, \pm 1, \pm 2$	0	No	α^4
Hyperfine	$0, \pm 1, \pm 2$	$0, \pm 1$	$0, \pm 1$	No	$\alpha^4(m/M)^2$

[a] Here α is the Sommerfeld fine-structure constant, m is the mass of the electron, and M is the proton mass.

continuum state. The quantum numbers L, S, J, and m_J represent constants of the motion for the discrete state, while L', S', J', and m_J' are the corresponding quantities for the continuum state. The parity of a state is defined as either even or odd according to whether $\sum_i l_i$ is even or odd, and the sum is taken over all electrons.

The selection rules for a given perturbation operator $\mathcal{H}'$ prescribe the values of $\Delta L = L' - L$, $\Delta J = J' - J$, etc., relating the initial discrete and final continuum states for which nonzero matrix elements are obtained. These are summarized in Table I for L–S coupling along with the relative decay rates evaluated by assuming that *all* interelectronic distances are of the order of a Bohr radius. The transition rates for the magnetic interactions are smaller than those for the Coulomb interaction by a factor of $1/\alpha^4 \approx 2 \times 10^8$ so that the magnetic autoionization lifetimes are characteristically of the order of 10^{-5}–10^{-7} sec. These lifetimes are long compared to typical radiative lifetimes so that a state will be truly long-lived only if it is also metastable against radiative transitions to lower-lying levels. It is clear that sharp optical lines can arise from transitions between states which are metastable against auto-ionization.

An energy-level diagram which is useful for discussing all of the alkali atoms is shown in Fig. 1. The atomic ground state ($^2S_{1/2}$) consists of a single s electron outside a closed shell, while the ground state of the single ion ($^1S_0$) is that of the neighboring rare-gas atom. The normal atomic spectrum, denoted by I or I^a, arises from excitation of the outer electron into higher quantum states, all of which are doublets since the spin of the closed core is zero. Two series of excited ion levels are formed depending on whether the excited electron and the residual "hole" have their spins parallel (triplet) or antiparallel (singlet).

We are concerned here with those states which may be formed by the excitation of a single electron from the outermost filled shell, and the spectrum resulting from these states is designated I^b. All such states in the alkali atoms have energies greater than the first ionization potential. The lowest I^b term is the doublet state in which the inner electron is raised to the same ns state as the valence electron. Above this level, both doublets and quartets may be formed. In the energy range below the first excited triplet state of the ion, any quartet states will be metastable against auto-ionization since the adjacent continuum levels are doublets, as can be seen in Fig. 1. Moreover, since there are no quartet levels in the I^a term sequence, the lowest quartet state will be metastable against radiation as well, for the selection rule $\Delta S = 0$ holds for electric dipole radiation. It should be noted that there are also states of higher multiplicity arising from the simultaneous excitation of two or more inner-shell electrons (excepting lithium, of course) which are metastable against auto-ionization as well as radiative decay.

1. Lithium

The first system of interest is the three-electron configuration, lithium, and the negative helium ion. Metastable quartet levels in He^- have been considered theoretically in some detail[12] in several attempts to find a bound level which would account for the observed production of negative helium ions in charge-exchange collisions.[4,13] A summary of the calculated energies of the lowest quartet states in lithium, including several recent results, is given in Table II (Refs. 14–18).

The lowest quartet levels are $(1s2s2p)\,^4P_J$ which are metastable against both auto-ionization and radiative decay. From Table I we see that the $^4P_{5/2}$ state is coupled to a continuum $[^1S_0(Li^+) + k^2 f_{5/2}]\,^2F_{5/2}$ state through the spin-spin interaction. The matrix elements for all other operators between the $^4P_{5/2}$ state and the continuum vanish. The $^4P_{3/2}$ and $^4P_{1/2}$ states are connected to continuum $^2P_{3/2}$ and $^2P_{1/2}$ states by the

[12] E. Holøien and J. Midtdal, Proc. Phys. Soc. (London) **A68**, 815 (1955); **90**, 883 (1967).

[13] V. M. Dukel'skü, V. V. Afrosimov, and N. V. Federenko, Zh. Eksperim. i Teor. Fiz. **30**, 792 (1956). [English transl.: Soviet Phys.—JETP **3**, 764 (1956)]; P. M. Windham, P. J. Joseph, and J. A. Weinman, Phys. Rev. **109**, 1193 (1958).

[14] Ta-You Wu and S. T. Shen, Chinese J. Phys. **5**, 150 (1944).

[15] S. T. Manson, Ph.D. thesis, Columbia University, 1966 (unpublished); private communication. See also J. L. Pietenpol, Phys. Rev. Letters **7**, 64 (1961). The lifetime obtained by Manson is based on a 15-parameter variational wave function and is believed to be more reliable than Pietenpol's result.

[16] F. Minn (to be published).

[17] E. Holøien and S. Geltman, Phys. Rev. **153**, 81 (1967). This reference contains previously unpublished work of A. W. Weiss.

[18] J. D. Garcia and J. E. Mack, Phys. Rev. **138**, A987 (1965).

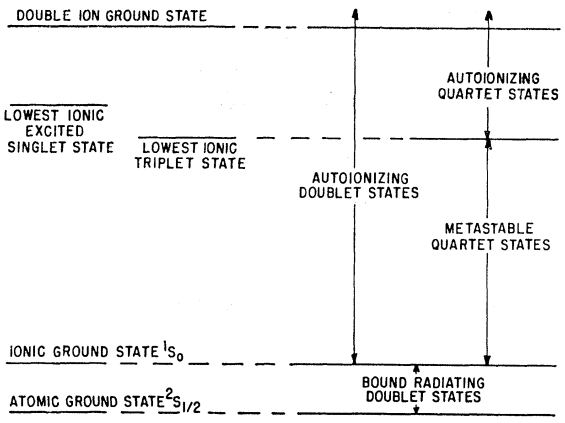

FIG. 1. General alkali atom energy-level diagram showing the range in which metastable auto-ionizing state may occur.

spin-orbit and spin-spin interactions, and in addition, in second order via the intermediate $(1s2s2p)^2P_{3/2}$ and $(1s2s2p)^2P_{1/2}$ states. Hence, the $^4P_{5/2}$ state is expected to have a longer lifetime than either the $^4P_{3/2}$ or $^4P_{1/2}$ states. Manson[15] has recently calculated the $^4P_{5/2}$ lifetime and obtained a value of 5.88×10^{-6} sec.

None of the other quartet states are metastable against radiative decay, and they all cascade to the lowest $(1s2s2p)^4P$ level. Since some of these transitions may be of interest in explaining several unidentified lines attributed to the LiII spectrum,[19] we indicate here the principal transitions:

$$(1s2p^2)^4P\text{–}(1s2s2p)^4P,$$
$$(1s2s3s)^4S\text{–}(1s2s2p)^4P,$$
$$(1s2s3d)^4D\text{–}(1s2s2p)^4P,$$
$$(1s2p3s)^4P\text{–}(1s2p^2)^4P.$$

2. Other Alkalis

The other alkalis may be similarly analyzed for metastable autoionizing states, except that theoretical estimates of energies and lifetimes are not available. The ultraviolet absorption spectra obtained by Beutler and his collaborators[20] during the 1930's provide energy values for some of the short-lived terms in the I[b] spectra of potassium, rubidium, and cesium. A list of the low-lying configurations which satisfy the autoionization metastability requirement is given in L–S coupling in Table III along with the energies of the lowest-lying states listed by Beutler. In a given configuration, the electrostatic energy is least for the states of highest multiplicity (Hund's rule), so that one would expect the quartet levels to lie below the doublets arising from the same configuration. In the case of Rb and Cs, Beutler identified, although in some cases tentatively, several lines terminating on ^4F and ^4P levels of total angular momentum quantum number J either $\frac{3}{2}$ or $\frac{1}{2}$. Optical excitation to these states is possible since the large spin-orbit interaction in these atoms breaks down the Russell-Saunders coupling scheme. In such cases the selection rules for autoionization are also modified and this is discussed below in Sec. II.C.

[19] G. Herzberg and H. R. Moore, Can. J. Phys. **37**, 1293 (1959). See also C. L. Pekeris, Phys. Rev. **126**, 143 (1962).

[20] H. Beutler and K. Guggenheimer, Z. Physik **87**, 176 (1933); **88**, 25 (1934); H. Beutler, *ibid.* **86**, 495 (1933); **91**, 131 (1934).

B. Excitation

Alkali atoms in the metastable quartet states may be produced by electron impact excitation of ground-state atoms. Since this excitation involves a change of multiplicity, the excitation function is characteristic of exchange collisions, i.e., the cross section attains its maximum value within a few electron volts of the threshold energy and then decreases very rapidly.

For lithium, Wu and Yu[21] have estimated the maximum cross sections for excitation of the corresponding doublet states using a Born approximation calculation. Their results indicate that the maximum cross sections for excitation from the inner shell are two or three orders of magnitude smaller than those for the excitation of the valence electron to the lowest excited atomic states. Furthermore, the cross sections are even smaller for the simultaneous excitation of two electrons or for other excitations corresponding to forbidden optical transitions. In general, the greater the degree of the "forbiddenness," the smaller will be the electron impact excitation probability. For example, their calculated values of the cross-section maximum for the two $(1s2s2p)^2P$ states are 3.4×10^{-19} and 1.9×10^{-18} cm^2. We shall use the lesser of these values as an order-of-magnitude estimate of the ^4P excitation cross section. This estimate may be in error by a factor of ten.

TABLE II. Theoretical estimates of the energies (in eV) of the low-lying quartet states in lithium.

Lithium level	a	b	c	d	e	f
$(1s2s2p)^4P$	57.99	57.68	57.52	57.47	55.47	57.44
$(1s2p2p)^4P$	61.42	···	···	60.74	59.67	60.76
$(1s2s3p)^4P$	···	···	···	61.33	61.75	···
$(1s2s3s)^4S$	···	···	···	61.69	61.11	61.65
$(1s2s3d)^4D$	···	···	···	···	61.80	62.73
$(1s2p3s)^4P$	···	···	···	62.77	63.17	···
$(1s2s4s)^4S$	···	···	···	63.18	···	···

[a] Ta-You Wu and S. T. Shen, Ref. 14 (three-parameter hydrogenic orbitals wave function).
[b] S. Manson, Ref. 15 (15-parameter Hartree-Fock-type wave function).
[c] F. Minn, Ref. 16 (15-parameter configuration interaction wave function).
[d] E. Holøien and S. Geltman, Ref. 17 (Hylleraas-type variational wave functions).
[e] J. D. Garcia and J. E. Mack, Ref. 18 (screening parameter evaluation).
[f] A. W. Weiss, values quoted in Ref. 17 (configuration interaction wave function).

[21] Ta-You Wu and F. C. Yu, Chinese J. Phys. **5**, 162 (1944)

TABLE III. Lowest I^b terms in the alkali spectra.

Element	Low-lying quartet states	Lowest doublets observed by Beutler[a]	Quartets identified by Beutler[a]
Na	$(2p^5 3s3p)\ ^4D$		
	$(2s2p^6 3s3p)\ ^4P$		
K	$(3p^5 4s3d)\ ^4F$	$(3p^5 4s4s)\ ^2P_{3/2}$, 18.7 eV	
	$(3p^5 4s4p)\ ^4D$		
	$(3p^5 4s5s)\ ^4P$		
Rb	$(4p^5 5s4d)\ ^4F$	$(4p^5 5s5s)\ ^2P_{3/2}$, 15.3 eV	$(4p^5 5s4d)\ ^4F_{3/2}$, 18.2 eV
	$(4p^5 5s5p)\ ^4D$	$(4p^5 5s4d)$, 17.2 eV	$(4p^5 5s6s)\ ^4P_{3/2}$, 18.8 eV
	$(4p^5 5s6s)\ ^4P$		$(4p^5 5s6s)\ ^4P_{1/2}$, 19.5 eV
Cs	$(5p^6 6s4f)\ ^4G$	$(5p^6 6s6s)\ ^2P_{3/2}$, 12.3 eV	$(5p^6 6s7s)\ ^4P_{3/2}$, 15.4 eV
	$(5p^6 6s5d)\ ^4F$	$(5p^6 6s5d)$, 14.1 eV	$(5p^6 6s5d)\ ^4F_{3/2}$, 16.1 eV
	$(5p^6 6s6p)\ ^4D$		$(5p^6 6s8s)\ ^4P_{3/2}$, 16.2 eV
	$(5p^6 6s7s)\ ^4P$		

[a] Reference 20.

C. Breakdown of L-S Coupling

We have previously indicated the relevance of the breakdown of L–S coupling to the absorption spectra observed by Beutler. Even in the case of lithium, the effect of the spin-orbit interaction on the auto-ionization rate is not negligible owing to the large difference in the lifetimes of the quartet and doublet terms of the configurations of interest. For instance, the $(1s2s2p)^2P$ states in lithium have lifetimes of the order of 10^{-14} sec while the quartet lifetimes are of the order of 10^{-5} sec. A small amount of mixing of the doublets and quartets will thus have a sizable effect on the lifetimes of the quartet levels. In the case of interest, the spin-orbit energy is of the order of 1 cm^{-1} while the electrostatic splittings between ^4P and ^2P states are of the order of 10^4 cm^{-1}, so that the doublet-quartet mixing amplitude is of the order of 10^{-4}. Hence, the decay rate due to mixing alone is of the order of 10^6 sec^{-1} and is comparable in magnitude to the decay rate due to direct coupling of the quartets to the continuum. In the heavier alkalis this mixing is even greater.

In all of the cases of interest, the quartet state of highest total angular momentum ($J=L+S$) is necessarily a pure quartet state and can decay only via the spin–spin interaction. All of the other quartet states ($J=L+S-1, \cdots, |L-S|$) are strongly mixed with the short-lived doublets of the same configuration in addition to their direct coupling to the continuum via the same spin-orbit interaction, so that they almost certainly have much shorter lifetimes than the pure quartet state. The net effect of mixing and different coupling is that the quartet states with different values of total angular momentum have different lifetimes for auto-ionization.

D. Zeeman Quenching

In the case where the different fine-structure levels of a given state have different lifetimes, the coupling of these levels to one another by an external magnetic field will result in a modification of the lifetimes. This would be observed experimentally as a quenching of the longest-lived state by the magnetic field. This effect has been observed in all of the alkali atoms and will be discussed in detail in a subsequent paper.[10]

E. Stark Quenching

An electrostatic field may mix a metastable auto-ionizing level with a shorter-lived state of opposite parity and the same multiplicity. This mixing will reduce the lifetime of the long-lived state and result in a quenching of the metastable atoms. In the case of the metastable quartet states, the spin selection rule prohibits direct coupling to the doublet continuum. However, the electric field may couple the metastable state to an intermediate quartet state which is in turn coupled to the continuum by an internal magnetic interaction. For example, the $(4p^5 5s4d)^4F_{9/2}$ state of rubidium is coupled by an electric field to states of the form $(4p^5 np4d)^4G_J$, etc. and $(4p^5 5snf)^4G_J$, etc., some of which are strongly coupled to the continuum by the spin-orbit interaction.

According to the above argument we expect that the effective matrix element for Stark quenching is proportional to the product of the electric-field strength and the spin-orbit or other magnetic splitting for the electron configuration of interest. This implies that the Stark-quenching rate is proportional to the square of the field strength and that it is greater for heavy atoms than for light ones. Thus in the presence of an electric field we expect that the decay rate is given by

$$\gamma(\mathcal{E}) = \gamma_0 + K\mathcal{E}^2, \tag{3}$$

where γ_0 is the natural decay rate. The factor K includes the sum of the matrix elements and energy denominators for all of the intermediate states. It is important to recognize that the Stark-quenching constant K may be different for states having different

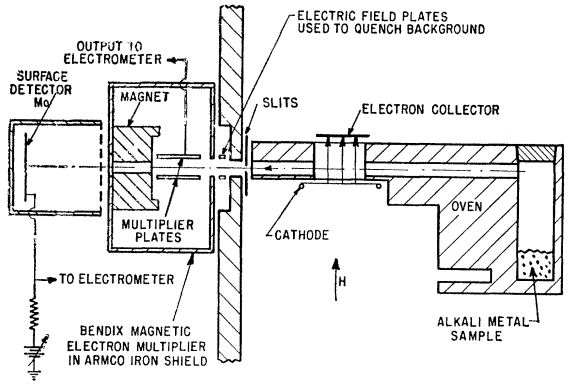

FIG. 2. Schematic diagram of the experimental arrangement for producing and detecting metastable auto-ionizing atoms.

values for the total angular momentum J and the magnetic quantum number m_J. This effect can be exploited for state selection through differential quenching. In addition, we expect that K will increase rapidly with the atomic number (Z).

III. EXPERIMENTAL ARRANGEMENT

A. Experimental Method

The basic experimental method used to investigate the states of interest is to produce a beam of metastable atoms by electron bombardment of neutral alkali atoms and then to measure the ion (or electron) current produced along the beam path because of auto-ionization. An atomic-beam experiment is possible since for atoms in states with microsecond lifetimes and moving with thermal velocity the decay length is of the order of a centimeter. Here we briefly describe the experimental arrangement and estimate the metastable ionization current at the detector.

The experimental arrangement shown schematically in Fig. 2 consists of two components, a source of the metastable atoms and an ionization detector. The source is a large-aperture atomic-beam oven with a suitable electron beam passing transverse to the alkali beam. If we neglect for the moment the angular distribution of the emerging atomic beam and the effect of bombardment recoil, the beam may be described as a current of N_0 particles per second with a characteristic v^3 thermal velocity distribution.

The detector, situated a distance x from the source, measures the number of charged particles, either ions or electrons, resulting from the auto-ionization of the metastable atoms over a given length. We shall assume that the detector is 100% efficient over several decay lengths so that all of the metastable atoms entering the detector decay within it. The measured current at the detector I_m is

$$I_m = N_m e, \tag{4}$$

where N_m is the number of metastable atoms per second entering the detector and e is the electronic charge. For a given velocity v, the number of metastable atoms reaching a distance x from the source in a solid angle $d\Omega$ is

$$N_m(x, v)\,d\Omega = N_0 \sigma F t_B \exp(-x/\tau v)\,d\Omega. \tag{5}$$

Here, σ is the excitation cross section in cm^2, F is the incident electron flux in electrons per sec cm^2, and t_B is the time spent by an atom in the bombardment region. For an electron current of I_c amperes passing through a slit of length L and width w, $F = I_c/Lwe$ electrons per sec cm^2, and $t_B = L/v$ sec. Integration over the velocity distribution gives for the ion current in a detector of infinite length

$$I_m d\Omega = \frac{2N_0 \sigma I_c}{\alpha^4 w} \int_0^\infty v^2 \exp(-v^2/\alpha^2) \exp(-x/\tau v)\,dv\,d\Omega, \tag{6}$$

where $\alpha = \sqrt{(2kT/M)}$ is the most probable velocity in the neutral atomic beam. The integral is evaluated numerically for the purpose of determining τ from the experimental data, but for our estimates we may neglect the velocity distribution and replace the second exponential in the integral by $\exp(-x/\tau\alpha)$. Then Eq. (6) becomes

$$I_m d\Omega = (N_0 \sigma I_c/\alpha w) \exp(-x/\tau\alpha)\,d\Omega \text{ A}. \tag{7}$$

Typical experimental parameters for a lithium source including a high-intensity electron gun are: $N_0 = 10^{16}$ atoms/sec, $I_c = 0.01$ A, $w = 0.025$ cm, $\alpha = 1.35 \times 10^5$ cm/sec. Manson's[15] value for the $(1s2s2p)\,^4P_{5/2}$ state lifetime is 5.88×10^{-6} sec. With an estimated value of $\sigma = 10^{-19}$ cm^2 for excitation to the $(1s2s2p)\,^4P_{5/2}$ state, the expected signals at distances of 3, 6, and 12 cm from the source are 5×10^{-13}, 2×10^{-14}, and 3×10^{-17} A, respectively. These currents are easily detectable with either conventional electrometer circuits or electron multipliers. The former were used in our initial studies[1] and the latter in the present work.

B. Apparatus

The experimental apparatus is contained in an 8-in.-diam stainless-steel vacuum envelope separated into two chambers for the source and detector. Each section is pumped by an 80-liter/sec mercury diffusion pump. The pressure in the detector region is consistently $\cong 10^{-7}$ Torr, while the source pressure varies from 10^{-7} to a few times 10^{-6} Torr. No evidence was found in any of our experiments for the collision quenching of a beam of metastable atoms at background pressures up to 10^{-5} Torr. The geometry of the system was designed so that a minimum source-to-detector distance of three centimeters is achieved while at the same time complete isolation is maintained between the two regions. The source and detector are described in detail below.

1. Source

The molybdenum oven and the integral electron gun are illustrated in Fig. 3. The oven is of standard

design. Attached to its front end is a molybdenum anode block with a 0.020-cm slit, one centimeter long, which defines the electron-bombardment region transverse to the atomic beam. The anode block also contains an extension of the 0.318-cm-diam oven canal, which when placed in position against the separating bulkhead in the vacuum chamber allows the atomic beam to enter the detector region directly but prevents stray electrons from the cathode from reaching the detector. If this is not done, the stray-electron background current completely masks any ionization current due to the decay of the metastable atoms.

A magnetic field of 1 kG, produced by an external electromagnet with its pole pieces extended into the vacuum envelope, serves to focus the electron beam through the bombarding slit as well as to constrain the motion of the electrons and the ions formed in the region of the slit. Electrons may reach the collector only by passing through the bombardment slit, which may be aligned with the magnetic field from outside the vacuum system.

The electron-gun components except for the anode are mounted on a ceramic support (boron nitride) which is fastened to the oven by means of three threaded rods on the side of the oven. Two electron-gun configurations have been used depending on whether the primary requirement for a given experiment was high-current density or high electron energy resolution. For high electron currents, an 0.018-cm-diam pure tungsten filament is used as a directly heated cathode in a triode configuration. Since the electron gun is magnetically focused, the filament is heated by a regulated 100-kc/sec current, but this results in an inductive voltage drop across the filament and an electron energy spread of the order of one electron volt. The current-voltage relationship approximately follows Child's law for space-charge-limited emission in a planar system. In the presence of the alkali beam, the emission is somewhat higher due to the partial neutralization of the electron space charge by the formation of positive alkali ions. Typical values of the bombarding current are 15–20 mA for lithium and about 8–12 mA for the other alkalis at the energies at which observations are made. The uncertainty in the determination of the electron energy with this electron-gun configuration is about 1 eV.

The other electron-gun arrangement is a tetrode configuration in which the electron source is an indirectly heated cylindrical oxide-coated cathode of the type used in the type-6C4 electron tube.[22] An accelerating grid biased six volts positive with respect to the cathode produces a constant current electron beam. As in the triode arrangement, the anode is at ground potential while the negative cathode voltage is varied to give the desired electron energy. The electron collector is kept at a fixed positive potential with respect to the anode.

[22] The authors wish to thank the Radio Corporation of America and the Raytheon Corporation for making available a generous supply of these cathodes and heaters.

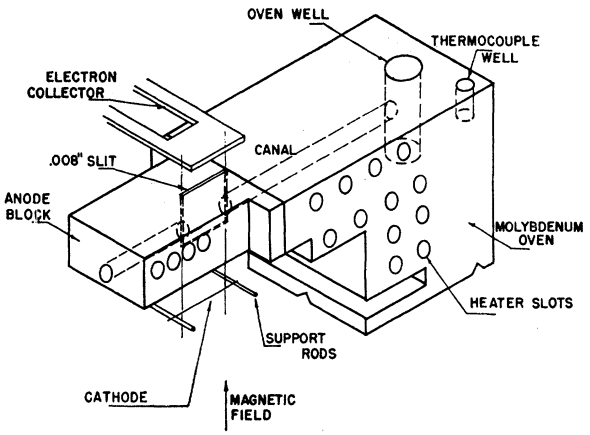

FIG. 3. Alkali oven and electron-gun assembly.

The currents obtained with this gun range from 0.1–0.2 mA, or a factor of 50–100 times smaller than that obtained with the triode. However, the average electron spread of a typical cathode is only 0.3 eV. The improved resolution permits the observation of structure on the excitation curves due to secondary excitations and also allows for an accurate determination of the excitation thresholds in conjunction with a suitable calibration of the energy scale. The oxide cathodes, however, are subject to poisoning from bombardment by alkali ions, and there is a noticeable decrease of electron emission and energy resolution within a few hours of activation of the cathode when the atomic beam oven is hot.

2. Detector

The basic detector consists of two parallel ion collecting plates. The atomic beam passes between the plates, and any ion-electron pairs resulting from auto-ionization are collected by the plates and appear as a current in an external return circuit. A small electric field is applied across the plates to enhance the ion collection efficiency. Our first observations of metastable auto-ionizing atoms were made with an arrangement of this type mounted in a grounded copper cage containing a large enough aperture to allow all of the atomic beam to enter the cage even at the largest distance used in this work. The entire cage is movable over a distance of 3 cm along the beam path by means of a bellows assembly on the end flange of the vacuum chamber, and this arrangement is used for time-of-flight measurements to determine the lifetimes of the metastable states. A copper honeycomb klystron grid mounted in a copper plate placed in front of the cage and biased positively with respect to ground serves to repel any remaining ions in the beam. The electrometer circuit used is of the Penick type[23] with a Victoreen VX-41a tetrode and an input resistance of 2×10^{11} Ω, both of which are enclosed in the vacuum system which acts as an electrostatic shield.

[23] D. B. Penick, Rev. Sci. Instr. **6**, 115 (1935).

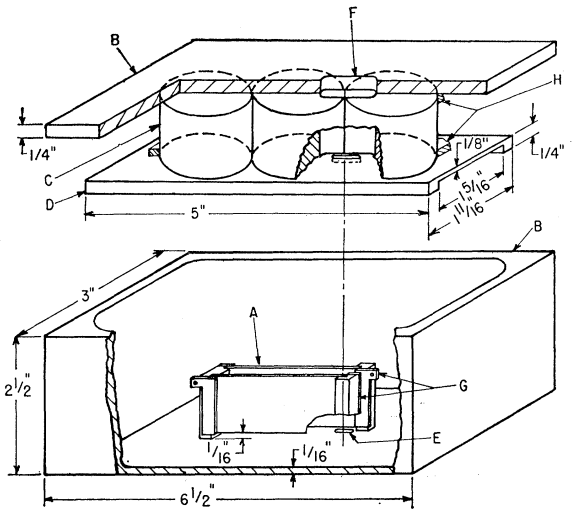

FIG. 4. Magnetically shielded resistance strip multiplier. A—Field and dynode strip assembly. B—Magnetic shield (Armco). C—Permanent magnets (Alnico V). D—Pole piece (Armco). E—Beam entrance slit. F—Exit slit. G—Clamps to replace grid and cathode assembly (stainless steel). H—Magnet and pole piece locating plates.

More sensitive detection is achieved with a Bendix model 306 magnetic strip electron multiplier. This device consists of parallel field and dynode plates and is ideally suited for our purpose. The conditions of our experiment, however, require slight modifications to the original unit. In order to prevent interaction of the magnetic field in the multiplier with the other magnetic fields present in the apparatus, a new magnetic circuit was designed which permits proper operation of the multiplier within an iron shield. The original grid and cathode assembly on the multiplier have been removed, and the atomic beam is allowed to pass directly between the dynode and field strips near the input end of the multiplier. Electrons resulting from the autoionization occurring in the region between the two strips are accelerated to the dynode strip by a transverse electric field and initiate the multiplication process. The ions formed also produce secondary electrons at the surfaces of the resistance strips, but these may be neglected as the production efficiency is very small at the energies to which they are accelerated.[24]

The modified detector is shown in Fig. 4. The magnetic shield is a soft iron (Armco) box with $\frac{1}{4}$-in. walls, and the glass dynode and field strips are supported from the front wall of the box in the same manner as in the unmodified unit. Three 1.067-in. long by 1.687-in. diam cylindrical Alnico V magnets produce the magnetic field, and the iron casing is utilized as a magnetic return path. An iron pole piece is shaped so as to give a field of modest uniformity over the multiplication region. The production of photoelectrons at the pole piece has been reduced by cutting a large exit slit through the pole piece, magnets, and back wall to allow any photons in the beam to pass completely through the detector.

The field in the multiplication region is approximately 300 G and is uniform to better than 10% over this region. As the magnetic field distribution is similar to that of the original multiplier, the gain and other performance characteristics are also the same. An external field of 300 G produces a field of less than 3 G within the shield while the leakage field outside the shield arising from the multiplier magnets is less than three gauss. Single electron pulses have been observed with time duration of the order of five nanoseconds and a charge multiplication of about 10^6 with 2000 V applied to the multiplier.

The multiplier is provided with both dc and ac outputs. The dc output is connected via an electrometer circuit to a pen recorder and may be used to determine the metastable excitation function directly. However, in many cases it is desirable to enhance the metastable signal with respect to any background present. This is done by modulating the electron beam energy by a few electron volts at some convenient frequency (in our case, 280 cps) and amplifying only the 280-cps component of the ac output from the multiplier. The output of a "phase-sensitive" or "lock-in" amplifier is then proportional to the derivative of the excitation function and is a maximum at the point of greatest slope. Of course, if the background also results from an energy-dependent atomic excitation, it will also give rise to a signal in the lock-in detector. In our experiments the background signals, sometimes several times larger than the metastable signals, are energy dependent, but have very gradual slopes at the metastable excitation energies so that the metastable signal near threshold can be effectively separated from the background.

It was found that the background can be greatly reduced by allowing the beam to pass through an electric field before it enters the detector. Condenser plates are mounted on the front of the detector for background suppression. These plates are separated by about 0.062 in. and extend about 0.125 in. along the beam. Background suppression is discussed in detail below.

3. Surface Detector

It is necessary to confirm that the observed signal attributed to auto-ionization is not due to photoelectrons produced by scattered photons or electrons from the surface Auger de-excitation of nonauto-ionizing metastable atoms or molecules which may have been scattered into the detector. In particular, one might expect ultraviolet radiation from excited states of the alkali ions to be produced at electron energies slightly above those of the metastable auto-ionizing states. It should be noted that in an atomic-beam experiment, the photon distribution will be essentially isotropic with respect to the electron-bombardment region while

[24] P. M. Waters, Phys. Rev. 111, 1053 (1958).

the atomic beam is contained in a small solid angle defined by the geometry of the oven and bombardment region and by the distribution of recoil velocities. Hence, photon background will be important only if the cross section for excitation of radiating ion states is much greater than that for the production of metastable atoms. A comparison of the excitation function for the current observed at a metallic surface detector placed behind the autoionization detector with that of the latter is sufficient to determine if the photon or metastable atom background is of importance.

A more important use for the surface detector is in the calibration of the electron energy scale by comparison with the known excitation thresholds for certain metastable or radiating atomic or molecular states. We have used both molybdenum and magnesium surface detectors, mounted in the copper detector cage 10 cm behind the detector entrance aperture. The plate is biased negatively with respect to ground so that the ejected electrons appear as positive incident current which is measured with a second electrometer tube circuit mounted inside the vacuum chamber.

4. Stern-Gerlach Experiment

A magnetic-deflection experiment serves to differentiate any signal due to photons from that due to the autoionization of paramagnetic atoms since the latter would be strongly deflected by an inhomogeneous magnetic field. It is also possible to obtain a positive identification of the energy levels involved if the Stern-Gerlach peaks corresponding to separate m_J states can be resolved and the value of g_J measured.

The short decay lengths of the metastable atoms require that the deflecting magnet be as short as possible. Owing to the narrow collimating and detector slits required by the geometry of the experiment, the beam intensity is reduced by a factor of 20 even before the added path length of the magnet is considered, and the intensity is further reduced at high magnetic fields where a large fraction of the metastable atoms is Zeeman quenched.[10] The actual geometry is shown in Fig. 5. The magnet is the same as described in Ref. 10 except that the pole faces are shaped to produce a strongly inhomogeneous field. The length of the field is one centimeter, and the over-all path length through the magnet assembly is 2.2 cm. The source slit, fitted to the exit canal of the electron-gun assembly, and the detector slit are both movable by means of bellows assemblies on the vacuum envelope. In order to compensate partially for the decrease in beam intensity, the oven temperature is run higher than the normal value.

IV. EXPERIMENTAL PROCEDURE

A. Excitation Function

Excitation functions of the metastable states are obtained by measuring the output from the Bendix multiplier as a function of the incident electron energy at constant current. The cathode potential is varied continuously at a rate of 3.33 V/min over the energy range of interest and is monitored by a digital voltmeter. The electrometer output is fed into a pen recorder so that the excitation function appears directly on the recorder. Recordings are taken with both increasing and decreasing bombarding energies. Any drift in the beam intensity or electron emission may be detected by comparison of the data from the up and down sweeps of a given run, and may be compensated for in the data reduction. This procedure also eliminates the sweep correction which would otherwise cause a shift of about 0.1 eV in the energy scale.

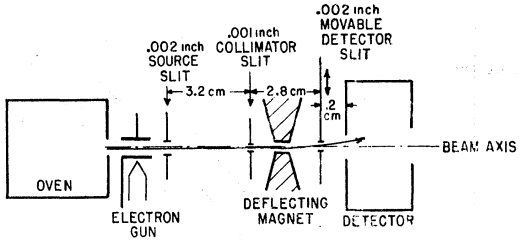

FIG. 5. Geometry of magnetic-deflection experiment.

In critical cases, the threshold energies are determined by taking point-by-point measurements of the signal at intervals of 0.1 eV. The excitation curves exhibit an onset which appears rounded because of the energy distribution of the exciting electrons. The threshold energies are found from an extrapolation of the linear portion of the excitation function to zero signal.

As noted in Sec. III B, the electron gun with an oxide-coated cathode is used for these measurements in order to obtain good energy resolution. For each run a new cathode must be used and each one is calibrated with reference to known excitation energies to eliminate any errors due to contact potentials, which may be as large as 1.5 eV. Atoms in the $(1s2s)^3S$ metastable state of helium (19.81 eV) and nitrogen molecules in the $a\ ^1\Pi_g$ and $A\ ^3\Sigma_u^+$ states[25] (threshold at 7.2 eV and a sharp peak at 12.3 eV) are used as calibration references and are detected by means of the Auger de-excitation at the surface detector. Helium or nitrogen gas is admitted to the system while the alkali oven is at normal operating temperature so that the calibration may also compensate for space charge effects due to ionization of the alkali beam. By measuring two thresholds at quite different energies, it is possible to confirm that the energy correction is actually independent of the electron energy as assumed. Only in the case of lithium where there is a large extrapolation to 57 eV can there be an appreciable uncertainty in this correction. An additional check on the energy scale is obtained from the appearance energies of the background as we shall see later.

[25] W. Lichten, J. Chem. Phys. **26**, 306 (1957); J. Olmsted, III, A. S. Newton, and K. Street, Jr., *ibid.* **42**, 2321 (1965).

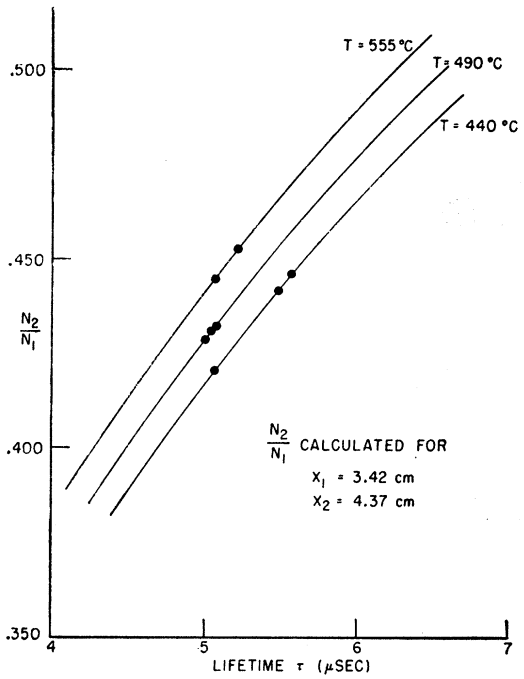

FIG. 6. Calculated value of the ratio of metastable signal at two distances from the source as a function of the lifetime τ. The three curves are for three oven temperatures at which data were taken in the case of Li, and the dots are the corresponding data points.

B. Lifetime

The lifetimes of the metastable states are determined by a time-of-flight method in which the ionization produced at different distances from the source is measured with the large-aperture movable detector. For Li, K, and Rb, the shape of the excitation function appears the same at different distances indicating that the apparent lifetime is independent of the bombarding energy.

In determining the lifetimes of the metastable states by this method, it is necessary to allow for the velocity distribution in the atomic beam. The electron bombarder has length L so that, if we assume a uniform distribution of electrons over this length, the number of metastable atoms surviving to a distance X from the center of the slit and into a solid angle $d\Omega$ is

$$\mathrm{I(X)d\Omega}=\frac{2N_0\sigma I_c}{\alpha^4 w}\int_0^\infty \frac{v^3\tau}{L}\exp(-v^2/\alpha^2)\exp(-\mathrm{X}/\tau v)\times[\exp(L/2\tau v)-\exp(-L/2\tau v)]d\Omega dv. \quad (8)$$

In terms of the dimensionless parameters $u=v/\alpha$ and $a=X/\tau\alpha$, the fraction of metastable atoms reaching a distance X is

$$\frac{N(X)}{N(O)}=\frac{4}{\sqrt{\pi}}\int_0^\infty u^3\exp(-u^2)\exp(-a/u)\frac{X}{aL}\times[\exp(aL/2uX)-\exp(-aL/2uX)]du. \quad (9)$$

The integral has been evaluated numerically with the aid of an IBM 7094 computer.

The lifetime is contained in the integrand as an undetermined parameter and may be deduced from the experimental data by a graphical procedure.[26] For this purpose, we measure the signals I_1 and I_2 at two different detector positions, X_1 and X_2, respectively, and compare the ratio I_2/I_1 to the theoretical values obtained from Eq. (9) for different assumed values of the lifetime. Figure 6 shows a plot of curves of I_2/I_1 versus τ obtained from Eq. (7) for three different temperatures at which data were obtained in the case of lithium. The plotted data points are averages of several measurements of I_2/I_1 for the two points X_1 and X_2 for which the curves are calculated.

C. Absolute Cross Section

Order-of-magnitude estimates of the absolute excitation cross section may be made by utilizing the lifetimes determined above and measurements of the metastable signal and the total neutral beam intensity. For the latter purpose, a 0.001-in.-diam hot-wire surface ionization detector, movable transverse to the atomic beam, is used. An alloy of 92% platinum and 8% tungsten is used for Li because of this element's high ionization energy (5.39 eV), while pure tungsten is used for the other alkalis. The data of Datz and Taylor[27] give an ionization efficiency of 20% at 1700°K for Li on the Pt-W alloy.

Several large uncertainties preclude more than an order-of-magnitude estimate of the absolute cross section. These are: (1) The efficiency of the autoionization detector may be less than the assumed value of 100%. (2) The effect of atomic recoil from electron bombardment is to reduce effectively the number of neutral atoms being bombarded, so that the value of N_0 which must be used in Eq. (6) to determine σ is actually less than the value determined from a measurement of the

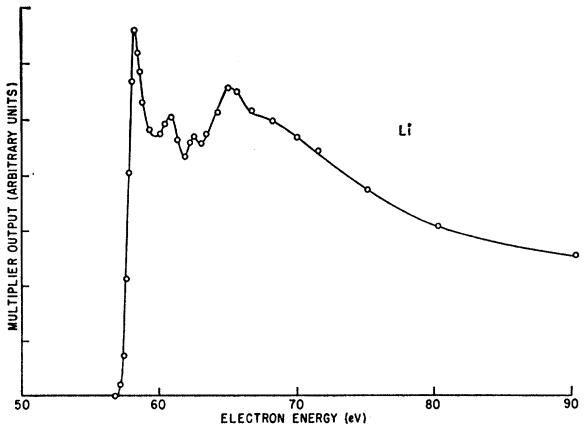

FIG. 7. Excitation function for metastable auto-ionizing states in lithium.

[26] W. Lichten, J. Chem. Phys. **26**, 306 (1957).
[27] S. Datz and E. H. Taylor, J. Chem. Phys. **25**, 389 (1956).

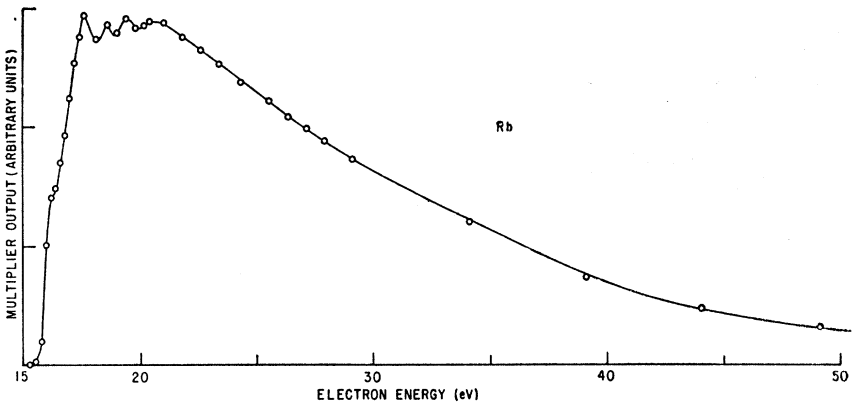

FIG. 8. Excitation function for metastable autoionizing states in potassium.

neutral beam intensity. (3) The efficiency of the hot-wire detector may be different from the value given by Datz and Taylor.

V. RESULTS AND DISCUSSION

A. Excitation Function, Lifetimes, and Cross Sections

1. Lithium

The excitation function for lithium is shown in Fig. 7. The sharp onset at 57.3±0.3 eV, attributed to the $(1s2s2p)^4P$ state, reaches its maximum at 58.2 eV and then drops sharply. Two smaller sharp peaks having apparent thresholds at 59.9±0.3 eV and 61.9±0.3 eV are tentatively assigned to the next two quartet states on the basis of the calculated energies given in Table II. These states radiate to the $(1s2s2p)^4P$ state in a time short compared with their autoionization lifetimes. The final broad rise on the curve is probably a superposition of several unresolved states lying just below the $(1s2s)^3S$ series limit at 64.4 eV since the maximum of the excitation function lies within 1.0 eV of that limit and the remainder of the curve decreases smoothly.

We cannot exclude the possibility that the secondary peaks result from quantum-mechanical interference between the direct and indirect excitation amplitudes of the $(1s2s2p)^4P_{5/2}$ state. Such effects have been recently observed by Schulz and Philbrick[28] and by Chamberlain[29] in atomic helium. In the case of lithium, an interference of this type can result from the excitation of the ^5P state of Li^- arising from the configuration $(1s2s3snp)$ with $n\geq 3$, lying of the order of 0.1 eV below the parent $(1s2s3s)^4S$ state in Li. This compound Li^- state may rapidly autoionize to the $(1s2s2p)^4P$ atomic state and appear as a resonance in the metastable production cross-section curve.

The experimental energy value of 57.3±0.3 eV for the $(1s2s2p)^4P$ state is in excellent agreement with the upper bounds of Minn[16] of 57.52 eV, of Manson[15] of 57.68 eV, and of Holøien and Geltman[17] of 57.47 eV, and of Weiss[17] of 57.44 eV. The calculated value of Garcia and Mack[18] falls below the experimental result. The measured lifetime of the $(1s2s2p)^4P_{5/2}$ state is 5.1±1.0 μsec, and the maximum cross section, at 58.2 eV, is $10^{-(19\pm0.5)}$ cm^2.

Garcia and Mack[18] have attempted to identify several unassigned lines[19] in the spectrum of Li^+ as transitions between quartet states of the atom. From Table II it is clear that the large disparity between their calculated energy for the $(1s2s2p)^4P$ state and the experimental value (a difference of ≈1.5 eV) will lead to erroneous wavelengths for transitions which terminate on the $(1s2s2p)^4P$ state. Holøien and Geltman[17] have also attempted to identify several of these transitions. In Table IV we list possible assignments for the states responsible for the observed thresholds. We have chosen these assignments to be consistent with the theoretical estimates of Holøien and Geltman since we have no means for experimentally identifying the higher-lying states.

2. Potassium and Rubidium

The experimental results obtained with potassium and rubidium are similar as may be expected since the electron configurations are the same, except for the principal quantum numbers, for the two elements. The excitation curves are shown in Figs. 8 and 9 for K and Rb, respectively. Maximum cross sections are $10^{-(18\pm0.5)}$ cm^2 for both, and the measured lifetimes are 90±20 μsec for K and 75±20 μsec for Rb. The detector current is 200 times larger than that for lithium because of the

TABLE IV. Thresholds observed on the lithium excitation function.

Threshold	Energy (eV)	Tentative assignment
1	57.3	$(1s2s2p)\ ^4P$
2	59.9	$(1s2p^2)\ ^4P$
3	61.9	$(1s2s3s)\ ^4S$, $(1s2s3p)\ ^4P$
4	63.2	$(1s2s4s)\ ^4S$

[28] G. J. Schulz and J. W. Philbrick, Phys. Rev. Letters **13**, 477 (1964).
[29] G. E. Chamberlain, Phys. Rev. Letters **14**, 581 (1965).

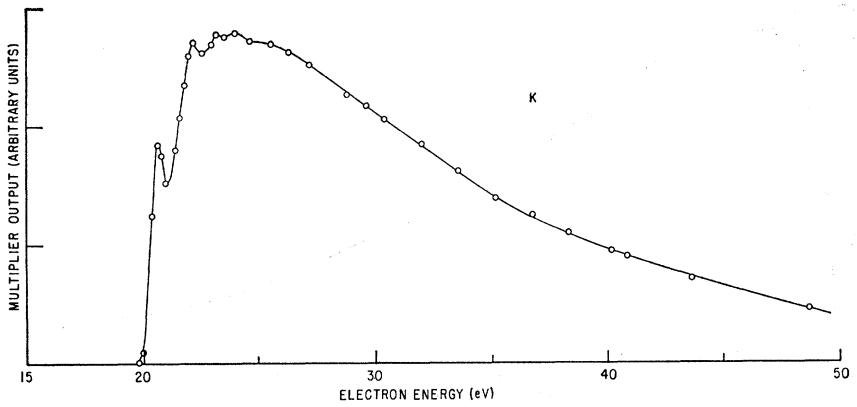

FIG. 9. Excitation function for metastable auto-ionizing states in rubidium.

longer lifetimes and larger cross sections. The structure on both curves consists of two principal onsets of almost equal amplitude and two or three secondary peaks which probably include unresolved states just below the series limit.

The onset energy of 19.9±0.3 eV for K lies above the two $(3p^54s^2)^2P$ states observed by Beutler and Guggenheimer[20] at 18.6 and 18.9 eV. Since the low-wavelength limit of their apparatus was at 600 A, or 20 eV, we may conclude that the energies of the doublet states arising from the $(3p^54s3d)$, $(3p^54s4p)$, and $(3p^54s5s)$ configurations lie above 20 eV and that the 19.9 eV onset represents the excitation of a quartet state of one of these configurations.

Our results for Rb may be compared with the energy levels established by Beutler[20] which include two $(4p^55s^2)$ doublet states at 15.3 and 16.15 eV and a series of $(4p^55s4d)$ states beginning at 17.2 eV. One of these states is a $(4p^55s4d)^4F_{3/2}$ term at 17.8 eV. If we assume that the first metastable threshold at 15.8±0.3 eV is the $(4p^55s4d)^4F_{9/2}$ metastable state, then this implies a fine-structure energy of the order of 2 eV or 16 000 cm^{-1} for this configuration. This is of the same magnitude as the multiplet level splittings of the parent $(4p^54d)$ states in Rb^+.

The assignment of states to the secondary thresholds on the excitation curves is not possible since the ordering of the levels is not known. In Rb, the second threshold may be either $(4p^55s5p)^4D$ or $(4p^55s6s)^4P$, depending on whether $5p$ lies above or below $6s$. As one goes higher in the periodic table, there is a greater depression of the s orbitals to energies below the energies of high angular momentum states with lower principal quantum number. Unfortunately, Beutler was not able to observe the excitation from the closed p shell to p or f orbitals owing to the $\Delta l=\pm1$ selection rule, so that the relative energies of the different configurations cannot be estimated. A $(4p^55s6s)^4P_{3/2}$ state was tentatively identified at 18.8 eV, 1.0 eV above the $(4p^55s4d)^4F_{3/2}$ level.

3. Cesium

As seen in Fig. 10, the excitation function for cesium is markedly different from those of potassium and rubidium, indicating that the ordering of the energy-level structure is different. A second threshold is observed 0.7 eV above the primary onset at 12.6±0.3 eV, but otherwise the over-all shape of the excitation curve is not the same. The maximum cross section is estimated to be between 10^{-20} and 10^{-19} cm^2. The excitation functions obtained at two different detector positions are of quite different shape. The low-energy peak decreases rapidly with distance while the broad rise starting near 19 eV remains constant. It is believed that the low-energy peak corresponds to the excitation of a metastable autoionizing state while the broad rise results from either scattered photons or possible metastable states of the Cs_2 molecule. The evidence supporting the hypothesis that this signal is not due to atoms is twofold: The signal at 50 eV is not affected by an inhomogeneous deflecting magnetic field, while the beam at 13.9 eV is deflected by a measurable amount (see Sec. V B). A null magnetic deflection for atoms can only occur in a state with zero total angular momentum. This is not possible for the Cs atom which has an odd number of electrons. Secondly, the surface-detector output gives an excitation function in which the main contribution has an onset corresponding to the lowest excited states of the ion, as shown in Fig. 11. The location of the Cs^+ states is indicated on the energy

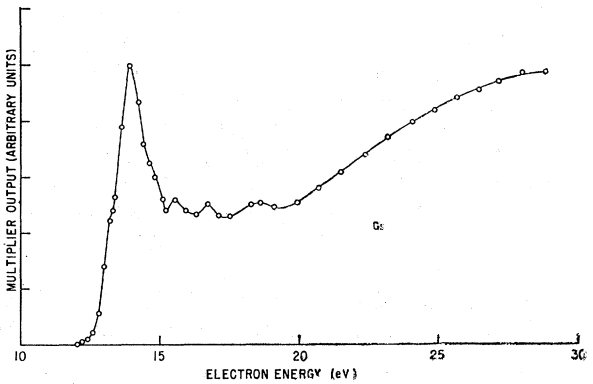

FIG. 10. Excitation function for cesium as obtained with the multiplier detector.

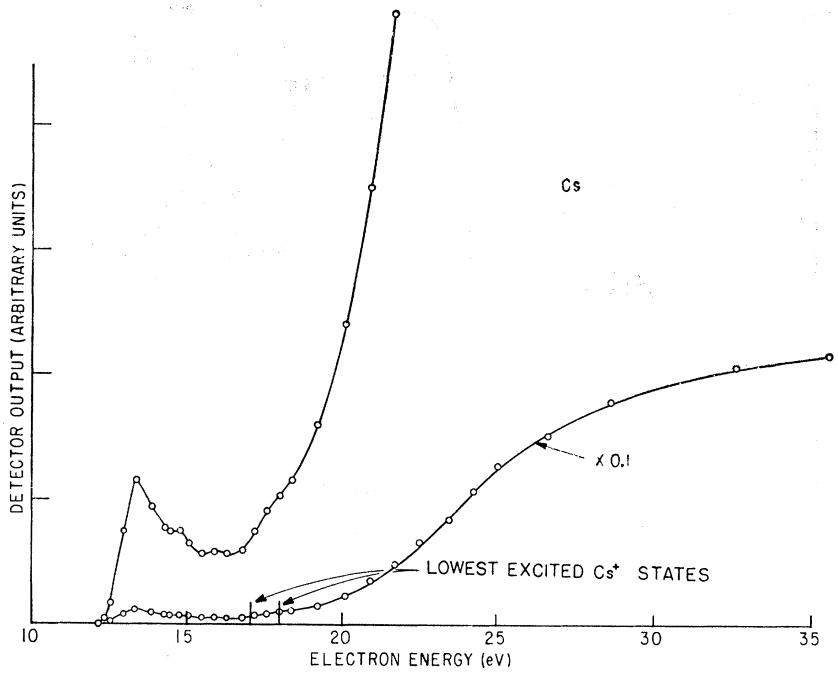

FIG. 11. Excitation function observed in the case of cesium with the surface detector.

scale. The excitation function for the ionic radiation is quite similar to the broad peak in the signal observed with the electron multiplier.

A small fraction of these ultraviolet photons produces photoelectrons at the surfaces of the multiplier plates or on the walls of the iron shield, and these are multiplied and appear in the output of the tube. Similar excitation functions, though slightly smaller in magnitude, are observed with the surface detector with K and Rb, and the thresholds can also be identified with the first excited states of the ion. In these instances the large metastable signal masks any photoelectron signal due to scattered ultraviolet light. The small threshold signal in Fig. 11 resembling the metastable excitation function may be due to the Auger de-excitation of metastable atoms reaching the surface detector or to photon emission from radiating atomic states of the type observed by Beutler.

The lifetime associated with the primary peak is 40 ± 15 μsec. Among the possible metastable states are $(5p^56s5d)\,^4F$, $(5p^56s6p)\,^4D$, $(5p^56s7s)\,^4P$, and $(5p^56s4f)\,^4G$. Beutler[20] identified several quartet terms in the absorption spectrum of Cs: $(5p^56s7s)\,^4P_{3/2}$ at 15.4 eV, $(5p^56s5d)\,^4F_{3/2}$ at 16.1 eV, $(5p^56s8s)\,^4P_{3/2}$ at 16.2 eV, and $(5p^56s7s)\,^4P_{1/2}$ at 16.7 eV. The closeness of these terms indicates the difficulty in making definite assignments to the thresholds observed on our excitation curve.

4. Sodium

The data on sodium are the poorest of the entire series, the low signal-to-noise ratio being the result of either a very small cross section or a lifetime a few times shorter than that of the metastable state in lithium. The observed signal, typically 10^{-17}–10^{-16} A, is not large enough to permit a lifetime determination with the movable detector. The excitation function of Fig. 12 also exhibits a signal due to the excitation of radiating states of Na^+ similar to that observed in cesium. The threshold energy, 31.8 ± 0.3 eV, is probably that of the $(2p^53s3p)\,^4D$ state, and is the only measurement of any of the Na I[b] terms.

B. Stern-Gerlach Experiment

The deflection patterns for a beam of metastable potassium atoms at several values of the deflecting magnet current are shown in Fig. 13. The widths at half-maximum intensity increase with increasing magnetic field, but distinct peaks are not observed even at the maximum field gradient. In the case of cesium, the signal-to-noise ratio is smaller, but it is possible to observe the deflection of the atoms excited at energies near the threshold energy. Unfortunately, in neither

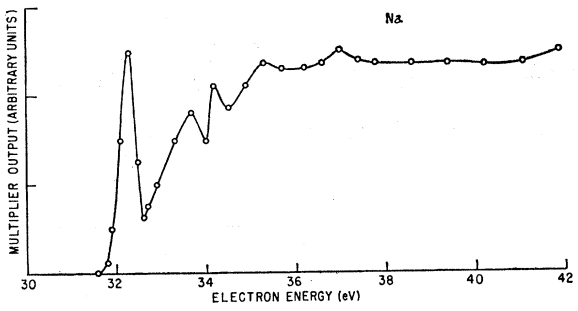

FIG. 12. Excitation function observed in the case of sodium with the multiplier detector.

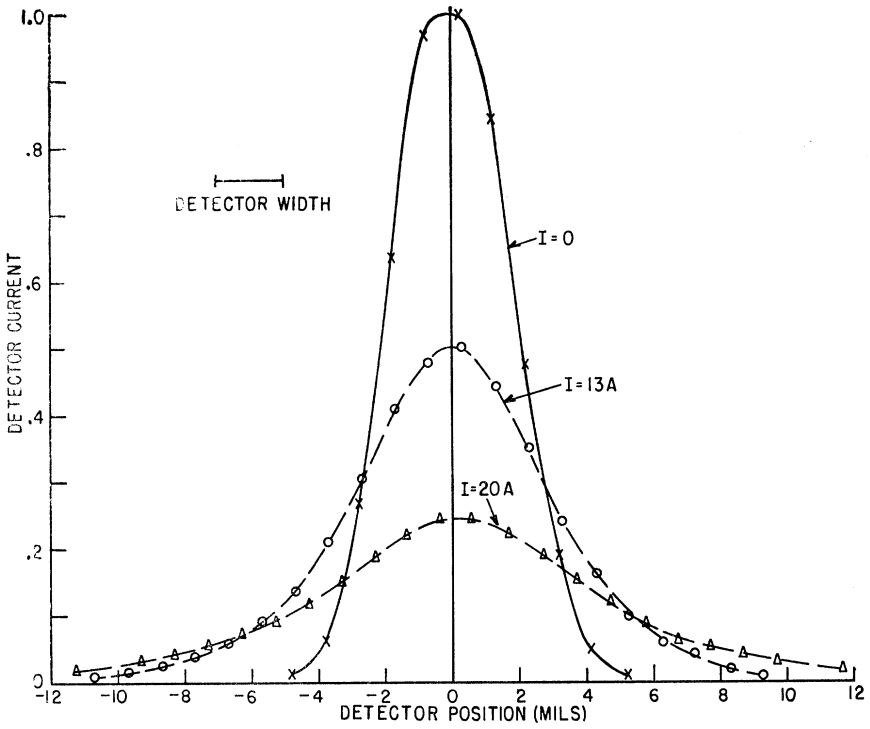

FIG. 13. Deflection patterns for a beam of metastable potassium atoms at different values of the current used to excite the deflecting magnet.

case is it possible to deduce from the data a positive identification of the angular momentum state of the atoms being deflected. However, the observed deflection indicates unequivocally that the observed effects arise from paramagnetic atoms and not from photons.

C. Stark Effect

Stark quenching is observed by interposing an electric field produced between a pair of polished stainless-steel plates, one centimeter long and separated by 2.5 mm between the source and the detector. The maximum voltage applied across the plates is 40 kV. According to the argument given in Sec. II.E, we expect that when the velocity distribution and a possible sum over quenchable states in the beam are neglected, the number of metastable atoms reaching the detector after passing through an electric field of length L is proportional to

$$\exp(-\gamma_a L/\alpha)\,\exp(-K\mathcal{E}^2 L/\alpha). \qquad (10)$$

Figure 14 shows a plot of $\ln(I_m)$ versus $\mathcal{E}^2$ for rubidium. The approximate linearity of this curve is consistent with our hypothesis. The small departure from linearity may be accounted for by the velocity distribution in the beam and by the differential quenching of the various sublevels. A similar effect is ob-

TABLE V. Threshold energies of the observed background signals.

Element	Background onset (eV)	Ionization potential (eV)
Li	5.2	5.390
K	4.2	4.339
Rb	3.9	4.176
Cs	3.4	3.893

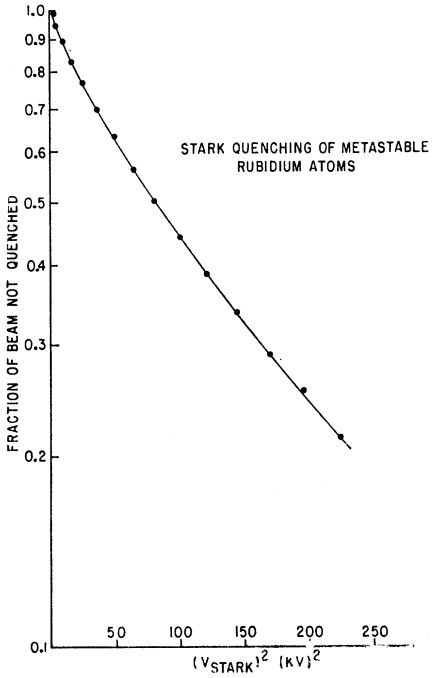

FIG. 14. Stark quenching of metastable rubidium atoms. The logarithm of the beam intensity is plotted as a function of the square of the quenching voltage. The spacing of the electric-field plates is about 2.5 mm.

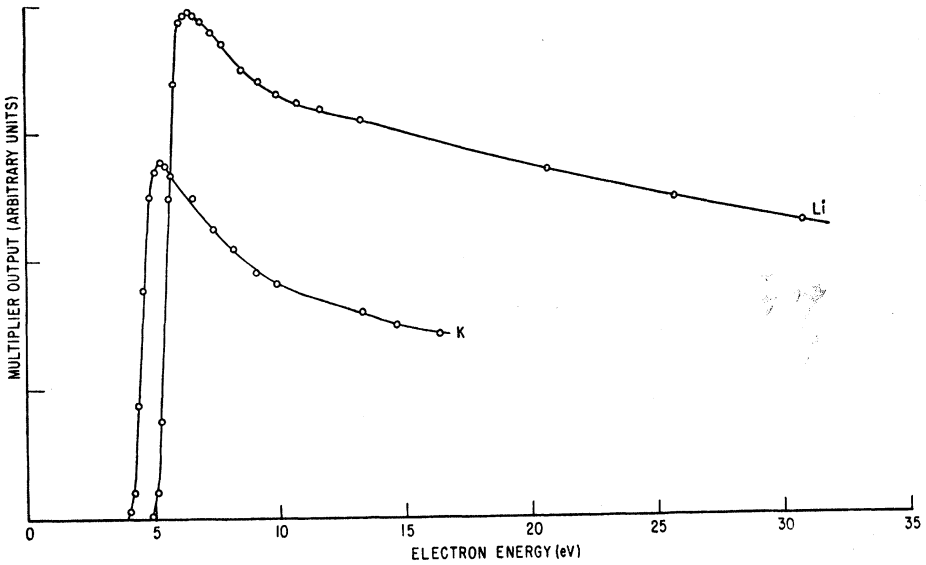

FIG. 15. Excitation function for background in the case of lithium and potassium.

served in potassium, but the fraction quenched is four times smaller than in rubidium, i.e., at a quenching voltage of 15 kV, the beam strength is attenuated to about 82% of its zero-field value. No detectable quenching of metastable lithium was observed even with quenching voltages up to 40 kV. This strong dependence of the Stark quenching on atomic number is consistent with our speculation that the quenching rate is proportional to the square of the matrix element of the spin orbit or other magnetic operator for the atom.

D. Background

In all of the experiments described above, a background signal is observed which is positively identified with electron excitation of the neutral alkali beam. An example of the excitation function associated with the background is shown in Fig. 15 for lithium and potassium. In lithium, the background signal is normally an order of magnitude greater than the signal from the autoionization of the metastable states, but in the other alkalis, it is negligible.

The experimental evidence suggests that the source of the background is the electric-field ionization of highly excited atomic states with radiative lifetimes greater than a few microseconds. This effect has been studied in hydrogen in experiments connected with ion injection into controlled thermonuclear machines.[30,31] In our experiment, the ionization is produced by the electric fields in the Bendix multiplier which are of the order of 10^3–10^4 V/cm over a path length of 3 cm. The calculation of electric-field ionization probabilities for hydrogen by Bailey, Hiskes, and Riviere[32] should be applicable to highly excited states of the alkalis. Their results give an ionization probability of 10^6 sec^{-1} at an electric-field strength of 2×10^3 V/cm for states of $n=20$ or higher. The natural lifetime for an $n=20$ level lies between 6×10^{-6} sec and 2×10^{-5} sec depending on the angular momentum of the state,[33] and this increases for higher quantum states. The energies of all of the excited states of Li with $n\geq12$ lie within 0.1 eV of the Li ionization potential at 5.39 eV.

All of these properties are consistent with the experimental data. The highly excited atoms which would be ionized by the electric field in the detector have sufficiently long natural lifetimes to reach the detector. The excitation cross sections for these states are smaller than those for the lowest excited levels, but may be comparable to the cross section for the production of the metastable autoionizing state. In lithium, the average lifetimes of these states are longer than the lifetime of the metastable state. This results in the relatively large background.

Two other experimental results are of importance. The threshold energies of the background excitation functions are measured by using the same energy calibration as that used for the determination of the energies of the metastable states. These are given in Table V, along with the spectroscopic values of the ionization potential for each atom.[34] To within the error of the measurement, all of the onsets, representing a superposition of many highly excited states, lie within

[30] K. H. Berkner, J. R. Hiskes, S. N. Kaplan, G. A. Paulikas, and R. V. Pyle, in *Atomic Collision Processes*, edited by M. R. C. McDowell (North-Holland Publishing Company, Amsterdam, 1964), p. 726.

[31] A. C. Riviere and D. R. Sweetman, in *Atomic Collision Processes*, edited by M. R. C. McDowell (North-Holland Publishing Company, Amsterdam, 1964), p. 734.

[32] D. S. Bailey, J. R. Hiskes, and A. C. Riviere, Nucl. Fusion **5**, 41 (1965).

[33] J. R. Hiskes, B. Tarter, and D. A. Moody, Phys. Rev. **133**, A424 (1964).

[34] C. E. Moore, *Atomic Energy Levels*, Natl. Bur. Std. Circ. No. 467 (U.S. Government Publishing and Printing Office, Washington, D.C., 1949).

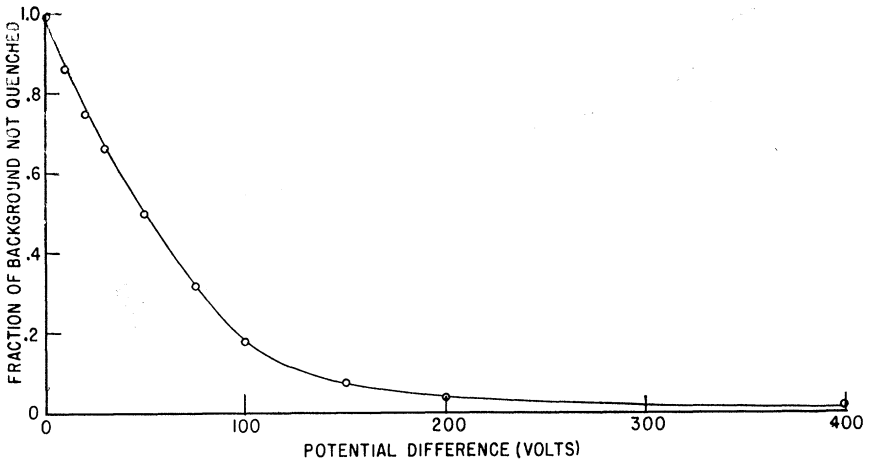

FIG. 16. Quenching of the background signal by an external electric field. The spacing between the quenching plates is about 1.5 mm.

0.2 eV of the ionization limit. Secondly, the highly excited atoms may be quenched out of the beam by an electric field before reaching the detector aperture. This results in a decrease in background in the detector output as shown in Fig. 16. In the experiments on the metastable auto-ionizing states, this background quenching field is kept at a convenient value to minimize the effect of the background on the data.

VII. CONCLUSION

The results of the present experiments may be summarized briefly. In Table VI are listed the threshold energies, lifetimes, and electron-bombardment production cross sections of the lowest metastable auto-ionizing state in each of the alkali elements. While these states have been identified on the basis of their decay mode, excitation energy, lifetime, and behavior in external electric and magnetic fields, it is important to note that positive spectroscopic identification has not been established. The long natural lifetimes of these states offer the attractive possibility for high-resolution radio-frequency spectroscopy as a means of determining the higher-order nuclear multipole contributions to the hyperfine interaction in the alkali elements. Such experiments will also provide a confirmation of our assignments of these states. Finally, we should point out that the existence of metastable auto-ionizing states in other elements may be of importance in understanding certain phenomena in plasmas.[35]

TABLE VI. Summary of results.

Element	Energy above ground state (eV)	Tentative assignment	Lifetime (μsec)	Electron bombardment production cross section (cm^2)
Li	57.3±0.3	$(1s2s2p)\ ^4P$	5.1±1.0	$10^{-(19\pm0.5)}$
Na	31.8±0.3	$(2p^53s3p)\ ^4D$	•••	•••
K	19.9±0.3	$(3p^54s3d)\ ^4F$	90±20	$10^{-(18\pm0.5)}$
Rb	15.8±0.3	$(4p^55s4d)\ ^4F$	75±20	$10^{-(18\pm0.5)}$
Cs	12.6±0.3	$(5p^56s7s)\ ^4P$ $(5p^56s5d)\ ^4F$ $(5p^56s4f)\ ^4G$	40±15	•••

ACKNOWLEDGMENTS

The authors would like to acknowledge the assistance of the entire staff of the Columbia Radiation Laboratory during the course of the experiment, in particular, Clifford Dechert and Israel Beller. Valuable discussions were held with Professor H. M. Foley and Dr. Steven Manson. We would also like to thank Morris Levitt and George Sprott for their contribution to various phases of the work.

[35] A. B. Prag and K. C. Clark, J. Chem. Phys. **39**, 799 (1963).